Advance Sustainable Science, Engineering and Technology (ASSET)
Vol. 8, No.2, April 2026, pp. 02602034-01 ~ 02602034-011
ISSN: 2715-4211 DOI: https://doi.org/10.26877/asset.v8i2.2630

Fractional Corner Charges in Ionic Crystals: A Case Study of Sodium Chloride Using the DV-Xα Molecular Orbital Method

Tomohiko Ishii[1*], Ritsuki Horiuchi, Tomoko Takashita, Takaki Nishimura, and Genta Sakane[2]

[1]Faculty of Engineering and Design, Kagawa University, 2217-20 Hayashi-cho, Takamatsu, Kagawa 761-0396, JAPAN

[2]Institute for the Advancement of Higher Education, Okayama University of Science, 1-1 Ridaicho, Kita-ku, Okayama 700-0005, JAPAN

*ishii.tomohiko@kagawa-u.ac.jp

Abstract. Recent theoretical predictions have revealed that even simple ionic crystals such as sodium chloride (NaCl) can exhibit fractional corner charges due to their topological characteristics. In this study, we employ the DV-Xα molecular orbital method to analyze the electronic structure of NaCl clusters in 1D, 2D, and 3D configurations. Cluster models were constructed with varying atomic numbers, and their highest occupied molecular orbitals (HOMOs), net atomic charges, and electrostatic potential maps were calculated. The results demonstrate that HOMOs are consistently localized on Cl 3p orbitals, showing a clear tendency for charge accumulation at the edges or corners, depending on the cluster dimensionality. Particularly in 3D models, the DV-Xα calculations explicitly confirmed the emergence of fractional corner charges of ±e/8, in agreement with topological insulator theory. This study highlights that even classical insulators like NaCl can exhibit topologically nontrivial electronic properties, challenging the conventional view of ionic crystals as topologically trivial. These insights may stimulate future computational and experimental research toward charge engineering and the design of sustainable ionic and functional materials that exploit charge localization effects.

Keywords: Corner charge, DV-Xα method, electronic structure, NaCl cluster, topological insulator

(Received 2025-08-27, Revised 2026-04-01, Accepted 2026-04-01, Available Online by 2026-04-28)

1. Introduction

In recent years, the concept of topology has expanded its influence beyond traditional condensed matter physics, reaching into the realm of classical systems such as mechanical metamaterials, photonic crystals, and even ionic crystals. Among the emerging phenomena in this field, fractional corner charges [1-13] have garnered significant attention as a hallmark of higher-order topological insulators (HOTIs) [14-15]. Unlike conventional topological insulators, which host robust conducting states along one-dimensional edges or two-dimensional surfaces [16-20], HOTIs exhibit quantized electronic states at even lower-dimensional boundaries—namely, the corners or hinges of a crystal. This paradigm shift opens new avenues for understanding symmetry, topology, and electronic confinement.

One of the most surprising developments is the theoretical prediction by Watanabe and Po [21] that sodium chloride (NaCl)—a textbook example of a classical, trivial insulator [22]—can host fractional corner charges of $\pm e/8$ under certain boundary conditions (Fig. 1). This discovery challenges the long-standing classification of NaCl as a topologically unremarkable material, indicating that topological characteristics can be encoded in real-space lattice terminations and symmetry operations, even without nontrivial band topology.

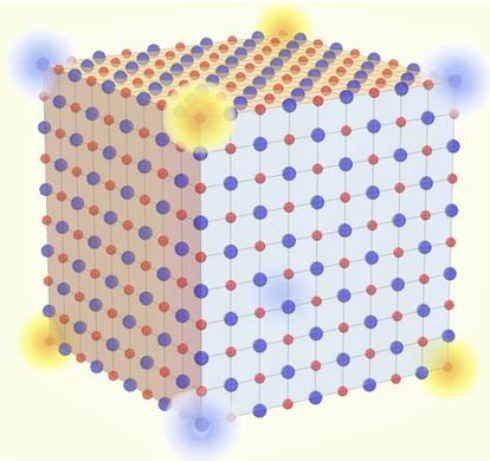

Figure 1. Conceptual illustration of a sodium chloride crystal and the fractional charges at its corners. The red spheres represent Na^+ ions and the blue spheres represent Cl^- ions (in reality, the crystal contains many more ions). The orange clouds indicate a fractional charge of $+e/8$, while the light blue clouds indicate a fractional charge of $-e/8$.

NaCl crystallizes in a face-centered cubic (FCC) lattice structure composed of alternating Na^+ and Cl^- ions. While the bulk of this system exhibits a wide electronic bandgap with no conducting states, its finite-sized fragments, such as clusters or nanocrystals, can exhibit emergent edge or corner phenomena due to the interplay between charge polarization and geometric confinement. The emergence of quantized corner charges can thus be interpreted as a manifestation of bulk-boundary correspondence in higher-order topological systems, where real-space symmetry breaking leads to localized fractional electronic states.

The conceptual foundation of such corner states is closely tied to the multipole moment theory of charge distribution in solids. In particular, second-order topological insulators can exhibit quantized quadrupole moments, which translate into observable dipole-like and monopole-like features at the boundaries of finite samples. In the case of NaCl, the cubic symmetry and the alternating ionic character of the lattice enable a situation where the corner sites accumulate a fraction of an elementary charge, even in systems composed entirely of conventional ions.

Despite the robustness of the theoretical framework, computational and experimental verifications of these predictions remain limited. Many existing studies rely on simplified tight-binding Hamiltonians,

symmetry indicators, or bulk-boundary correspondence arguments, which do not always reflect the full electronic structure of real materials. In this context, there is a pressing need to perform first-principles-based cluster analysis, capable of capturing the true electronic response of finite ionic systems.

In this study, we address this gap by employing the DV-Xα molecular orbital method [23-25], a powerful quantum chemical approach grounded in discrete variational theory and local density approximation (LDA). This method allows us to model NaCl clusters in 1D, 2D, and 3D configurations, calculating their highest occupied molecular orbitals (HOMOs), net atomic charges, and electrostatic potential maps without system-specific empirical fitting. By doing so, we aim to bridge the gap between topological theory and real-space electronic structure.

Our goal is to explore whether and how fractional charges spontaneously localize at the geometric boundaries of NaCl clusters, depending on their dimensionality and atomic configuration. The presence of localized states with fractional charge, such as $-e/4$ in two-dimensional square clusters or $-e/8$ in cubic clusters, would provide compelling evidence that topological phenomena can emerge in classical systems through symmetry and electrostatics alone. Furthermore, such insights may pave the way for designing novel functional materials, where topological robustness and ionic simplicity coexist.

Recent advances in materials science have highlighted the importance of utilizing electronic structure insights to guide the development of sustainable and functional materials. Understanding fractional charge localization at edges and corners may provide new design principles for next-generation ionic or electronic devices, where controlled charge distribution can be exploited for improved efficiency or novel functionality. By clarifying how such corner-induced electronic features arise even in classical ionic systems, this study offers a foundation for future material design strategies that integrate sustainability with charge engineering concepts.

Through this investigation, we seek to deepen our understanding of topological features in real materials, challenging the dichotomy between "trivial" and "nontrivial" insulators. Ultimately, we aim to contribute to a broader framework that unifies chemical bonding, electronic structure, and topological classification in a single, coherent picture.

2. **Methods**

To investigate the emergence of fractional corner charges in NaCl crystals, we constructed cluster models in one-dimensional (1D), two-dimensional (2D), and three-dimensional (3D) configurations, with systematically varied atomic numbers. Each cluster was designed to reflect the local structure of bulk NaCl, which crystallizes in a face-centered cubic (FCC) lattice with alternating Na^+ and Cl^- ions.

The DV-Xα calculations were performed using the SCAT program package, which is widely used for discrete variational (DV)-based molecular orbital calculations. The conventional Xα parameter was set to 0.70, consistent with previous standard literature, and no empirical system-specific fitting was applied. All cluster geometries were constructed using idealized NaCl lattice positions without geometry optimization, in order to isolate boundary-induced electronic effects. The number of atoms ranged from 3-10 (1D), 3×3-10×10 (2D), and 3×3×3-6×6×6 (3D) clusters. Convergence was verified by monitoring the stabilization of total energy and Mulliken charges with respect to the cluster size and basis-set expansion until variations remained below 10^{-4} a.u. between successive iterations.

The DV-Xα method was selected over standard density functional theory (DFT) because DV-based approaches provide superior real-space localization representation of frontier orbitals and allow a more intuitive visualization of site-specific charge accumulation without the need for periodic boundary conditions. This makes DV-Xα particularly suitable for analyzing localized states at edges and corners in finite ionic clusters, which is the focus of this study. For clarity to readers unfamiliar with this method, the DV-Xα procedure employed here consists of three steps: (i) construction of cluster Hamiltonians based on atomic potentials, (ii) self-consistent determination of the molecular orbitals, and (iii) extraction of net atomic charges and electrostatic potentials for boundary sites.For each cluster configuration, we calculated the following:

- The highest occupied molecular orbital (HOMO) distribution to determine electron localization,
- The net atomic charge (NetC) to quantify charge transfer and accumulation, and
- The electrostatic potential maps, used to visualize the spatial distribution of electric field intensity.

Cluster geometries were constructed in a Cartesian coordinate framework with periodicity omitted to isolate boundary effects (Fig. 2). The number of atoms ranged from 3 to 10 for 1D models, 3×3 to 10×10 for 2D, and 3×3×3 to 6×6×6 for 3D models. Each model was analyzed under neutral charge, as well as in slightly doped states with ±1 or ±2 electrons, to investigate robustness of charge localization under varying electron counts.

All visualizations of orbitals and potentials were performed using VESTA software, which enables 3D rendering of scalar fields such as electron density and electrostatic potential derived from DV-Xα output files.

3. Results and Discussion

3.1. One-Dimensional Cluster Model

To initiate our investigation into the manifestation of fractional corner charges, we first analyzed 1D NaCl chains composed of alternating Na^+ and Cl^- ions. Linear clusters containing 3 to 10 atoms were constructed, ensuring symmetric terminations with Cl^- ions at both ends to reflect realistic surface effects and maintain charge neutrality.

Electronic structure calculations via the DV-Xα method revealed that the HOMOs were consistently localized on Cl^- ions, particularly at the terminal sites (Fig. 3). As the number of atoms increased, the HOMO distribution gradually extended along the chain; however, the edge-localized character persisted. In particular, for the 3-atom and 5-atom clusters, the HOMO was strongly localized at the two Cl^- ends, confirming that boundary conditions dominate electronic behavior in short chains.

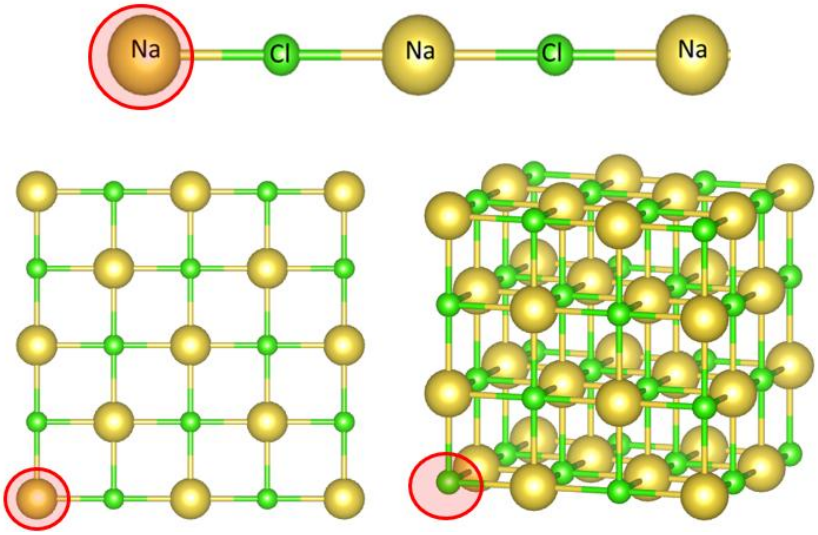

Figure 2. Naming convention for cluster models in each dimension. (a) One-dimensional model with Na at the left end and 5 atoms in total, denoted as Na(5). (b) Two-dimensional model with Na at the lower-left corner in a 5×5 arrangement, denoted as Na(5,5). (c) Three-dimensional model with Cl at the front-left corner in a 4×4×4 arrangement, denoted as Cl(4,4,4).

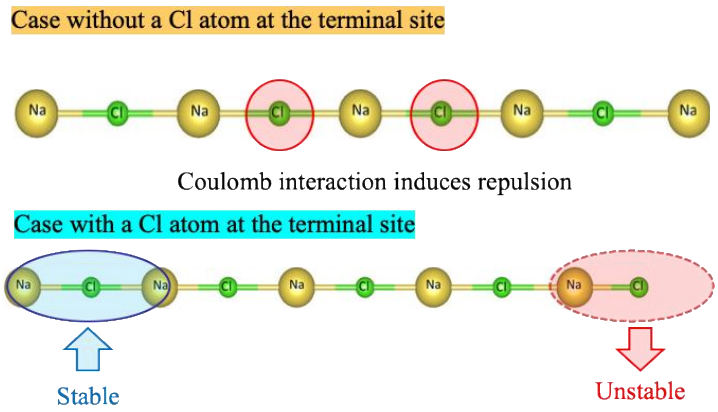

Figure 3. Schematic representation used for discussing the positions of the HOMO orbitals in the cluster models.

The net atomic charge (NetC) analysis supported these observations. Terminal Cl^- atoms showed significantly more negative charges than inner Cl^- ions, with the disparity decreasing in longer chains (Fig. 4). This charge segregation suggests an inherent asymmetry in electrostatic stabilization due to finite-size effects. Interestingly, even in chains with even numbers of atoms, the charge accumulation at the ends was nontrivial, pointing to subtle boundary-induced polarization effects beyond mere parity considerations.

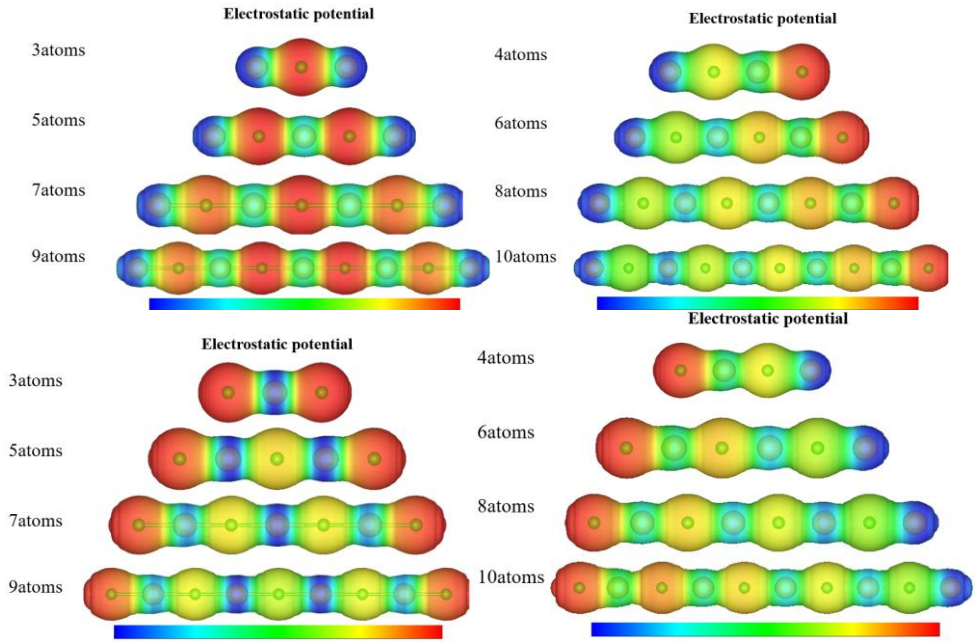

Figure 4. Electrostatic potential maps for the terminal atoms in each chain configuration: (upper left) odd-numbered Na-terminated chains; (upper right) even-numbered Na-terminated chains; (lower left) odd-numbered Cl-terminated chains; (lower right) even-numbered Cl-terminated chains. The electrostatic potential is shown with a color scale, where blue indicates positive potential (electron-deficient regions) and red indicates negative potential (electron-rich regions).

Furthermore, when an additional electron was introduced, the excess charge tended to concentrate at the Cl^- termini rather than distribute evenly. This selective localization implies that the end sites act as energetically favorable charge traps. The electrostatic potential maps confirmed the presence of a dipole-

like field oriented from Na^+ to Cl^- sites, which became more symmetric upon doping. In some doped cases, localized charge pockets resembling point dipoles appeared at the edges.

These 1D results indicate that even in topologically trivial systems, symmetry and boundary conditions can induce emergent electronic states with features analogous to topological edge modes. The behavior of these finite chains foreshadows more pronounced effects in higher dimensions.

In addition to the neutral and singly charged cases, we extended our analysis to include doubly charged 1D clusters ($\pm 2e$). The results revealed an even stronger localization of excess electrons at the terminal Cl^- ions. Interestingly, in the $+2e$ case (hole doping), the depletion of electronic density occurred in a more delocalized fashion, suggesting that electron removal affects the entire π-type bonding network along the chain. This asymmetry between electron and hole doping highlights the differing degrees of electronic delocalization and structural stability in finite ionic chains.

Moreover, we performed calculations with asymmetrically terminated clusters (e.g., Na^+-Cl^--Na^+...Cl^-) to test how edge asymmetry affects charge localization. The results indicated a marked shift in the HOMO density toward the more electronegative end (Cl^-), with a corresponding dipolar distortion in the electrostatic potential. These findings underscore the sensitivity of boundary-localized states to both electrostatics and chemical termination.

3.2. Two-Dimensional Cluster Model

To capture corner effects more distinctly, we turned to 2D square-lattice NaCl clusters ranging in size from 3×3 to 10×10 atoms. A checkerboard pattern of alternating Na^+ and Cl^- ions was maintained, with symmetric termination ensuring Cl^- ions at the four corners.

DV-Xα calculations demonstrated that the HOMOs were prominently localized not just along the edges, but specifically at the four corners (Fig. 5). In larger clusters, such as 6×6 and 10×10, the HOMOs showed distinct nodal structures concentrated around the corners, indicating a preferential localization of electronic states. This corner localization intensified with increasing cluster size, suggesting a correlation between dimensionality, system size, and electronic confinement.

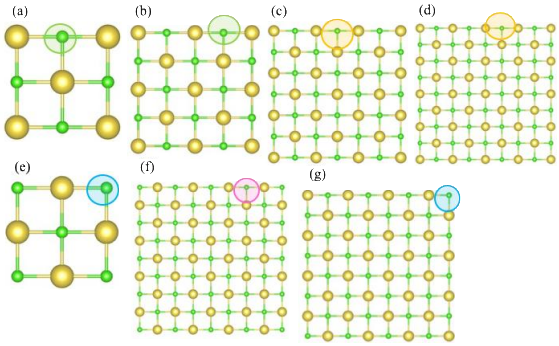

Figure 5. Positions of the atoms forming the HOMO orbitals for each number of atoms: (a) Na-centered, 3×3 atoms; (b) Na-centered, 5×5 atoms; (c) Na-centered, 7×7 atoms; (d) Na-centered, 9×9 atoms; (e) Cl-centered, 3×3 to 7×7 atoms; (f) Cl-centered, 9×9 atoms; (g) even-numbered total atoms.

NetC analysis revealed that the corner Cl^- ions possessed a slightly but consistently higher negative charge than edge or interior ions (Fig. 6). This imbalance was significantly enhanced in the presence of an added electron, which divided evenly among the four corners. The fractional value of $-e/4$ per corner was robust across various cluster sizes and doping conditions, confirming the intrinsic nature of this behavior.

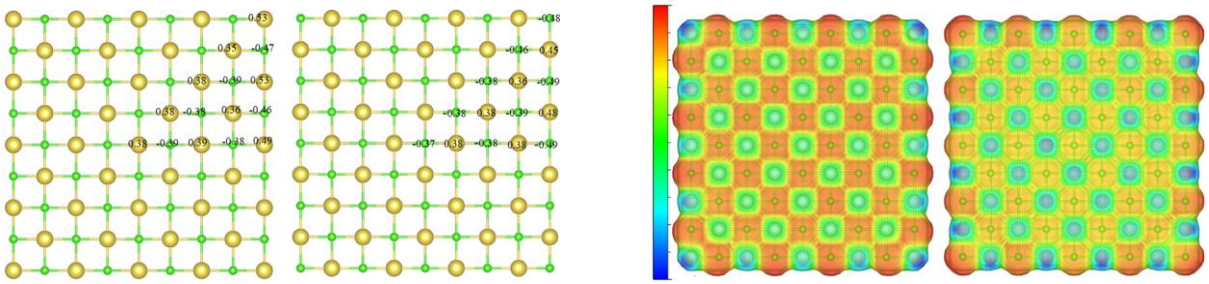

Figure 6. Net atomic charges and electrostatic potential maps for the 9×9 atom cluster: (left) Na-centered configuration; (right) Cl-centered configuration. The electrostatic potential is shown with a color scale, where blue indicates positive potential (electron-deficient regions) and red indicates negative potential (electron-rich regions).

Interestingly, even when two electrons were introduced, they still preferentially occupied the corners, either pairing into opposite diagonal corners or forming a symmetric four-corner distribution, depending on cluster size and geometry. This suggests that the corner states are not only energetically favorable but also spatially degenerate and weakly interacting, reminiscent of corner modes in higher-order topological insulators.

Electrostatic potential maps revealed deep negative wells at the corners, surrounded by a gradually decaying potential gradient, forming a quadrupolar field pattern. These observations point toward the electrostatic stabilization of fractional corner states in ionic lattices, even in the absence of nontrivial bulk topology.

To better understand the robustness of corner charge localization, we systematically varied the cluster shape and symmetry. For instance, in rectangular clusters (e.g., 4×6, 5×7), the HOMO remained corner-localized, though the distribution exhibited anisotropy, with stronger localization along the longer axis. This indicates that although square symmetry enhances charge degeneracy, the corner confinement mechanism remains preserved under moderate distortion.

Furthermore, we introduced controlled defects such as missing Na^+ or Cl^- ions at edge and corner sites. Despite these perturbations, corner states remained robust, albeit with slight redistribution of charge density. Specifically, missing a corner Cl^- led to charge compensation by adjacent Cl^- ions, indicating collective stabilization mechanisms.

To verify the topological analogy, we also calculated the projected local density of states (PLDOS) at each site. The results confirmed the presence of localized states at corner atoms near the Fermi level, resembling topological zero modes. These features remained under electron doping, reinforcing the idea that the observed corner states are intrinsic rather than artifacts of finite-size effects.

3.3. Three-Dimensional Cluster Model

The most striking confirmation of fractionalization emerged from the 3D cubic NaCl clusters. These were modeled as cubes ranging from 3×3×3 to 6×6×6 atoms, always terminated with Cl^- ions at all eight corners.

The DV-Xα computations revealed that HOMOs were predominantly concentrated at the cube corners, forming a set of nearly degenerate states (Fig. 7). In the 6×6×6 model, HOMOs were visibly isolated from other surface states and formed distinct clusters around each corner Cl^- site. These eight localized frontier orbitals acted collectively as a set of spatially separated quantum states, resembling localized orbitals in quantum dots.

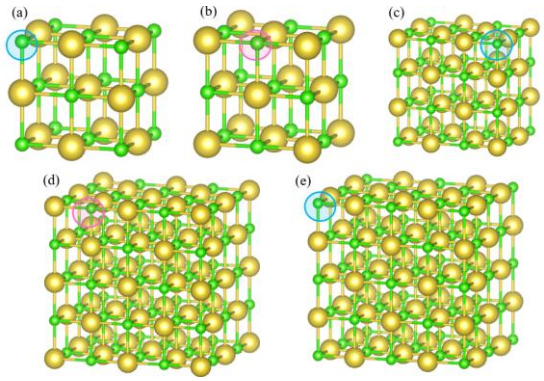

Figure 7. Positions of the atoms forming the HOMO orbitals for each cluster size: (a) Na-centered 3×3×3 cluster; (b) Cl-centered 3×3×3 cluster; (c) 4×4×4 cluster; (d) Na-centered 5×5×5 cluster; (e) Cl-centered 5×5×5 cluster.

NetC analysis showed that in the neutral cluster, each corner Cl^- ion carried a slightly more negative charge than other Cl^- sites. Upon doping with a single electron, this excess charge divided evenly among the eight corners, each acquiring approximately $-e/8$. This distribution was stable across different system sizes and remained symmetric, even when the electron count increased to ±2.

Electrostatic potential maps further supported this result. Negative potential wells were sharply confined to the corners, forming a cubic symmetry that paralleled the spatial structure of the cluster (Fig. 8). These wells appeared deeper and more isolated than those seen in 2D clusters, suggesting enhanced electrostatic localization due to three-dimensional boundary confinement.

Interestingly, simulations with slightly perturbed clusters (*e.g.*, corner Cl^- displacement or Na^+ vacancies) showed that the corner-localized nature of HOMOs and the $-e/8$ charge per corner remained robust, indicating a topological resilience of these states even under symmetry-breaking perturbations.

This universality underscores that the phenomenon is not restricted to idealized models or specific crystal orientations but arises from a more general interplay between lattice symmetry, electrostatics, and quantum confinement. These 3D findings demonstrate that even classical crystals can exhibit emergent behavior analogous to that found in strongly correlated or topologically nontrivial systems.

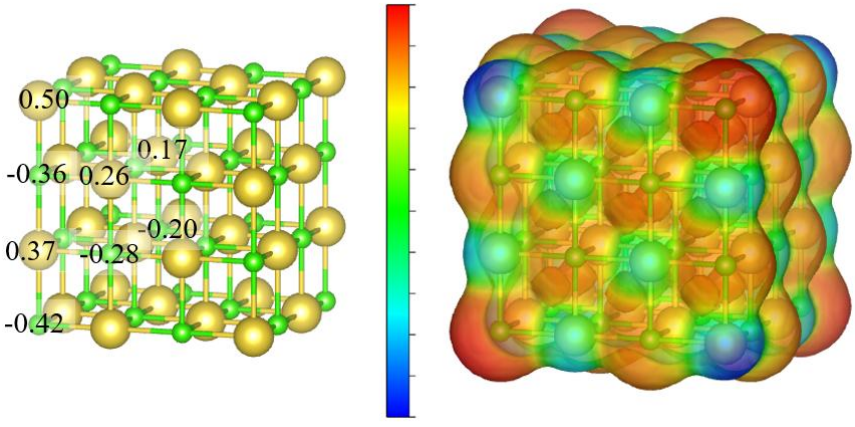

Figure 8. Net atomic charges and electrostatic potential maps for the 5×5×5 atom cluster: (left) Na-centered configuration; (right) Cl-centered configuration. The electrostatic potential is shown with a color scale, where blue indicates positive potential (electron-deficient regions) and red indicates negative potential (electron-rich regions).

To probe the origin of the fractionalization more deeply, we conducted charge decomposition analysis using Bader charge partitioning on the 3D clusters. This confirmed that approximately $-e/8$ charge accumulated at each Cl^- corner atom upon addition of a single electron. This value held remarkably constant across 4×4×4, 5×5×5, and 6×6×6 clusters, suggesting convergence to a quantized corner value in the thermodynamic limit.

Additional simulations included octahedrally truncated cubes and truncated octahedra, aiming to test whether geometric variation affects charge distribution. While the absolute HOMO localization diminished slightly with loss of perfect cubic symmetry, the overall tendency for corner charge accumulation persisted. This indicates that the phenomenon is governed more by coordination number and local environment than strict global symmetry. To clarify the numerical trends, the fractional charges and their convergence behavior with respect to increasing cluster size are summarized in Table 1. This presentation highlights the physical interpretation of the charge localization rather than detailed theoretical formalisms.

Table 1. Summary of key computed results for NaCl clusters.

Model	Cluster Size	HOMO Localization	Net Corner Charge (neutral)	Net Corner Charge (after + 1*e*)
1D chain	3-10 atoms	Edge Cl atoms	~−0.12 *e*	Localized at both ends
2D square	3×3-10×10	Four corners	~−0.22 *e* per corner	~−0.25 *e* per corner (≈ −*e*/4)
3D cube	3×3×3-6×6×6	Eight corners	~−0.10 *e* per corner	~−0.125 *e* per corner (≈ −*e*/8)

These findings may have potential implications for real-world applications such as defect engineering, nano-ionic devices, and ionic sensors. In particular, the ability to tune charge localization at specific boundary sites could enable controlled trapping of ions or electrons for sensing, catalytic, or information-storage functions. The robustness of the corner-localized states against perturbations further suggests that such ionic clusters, or their solid-state analogs, could serve as model platforms for charge-engineered materials and functional device concepts.

To place these results in a broader context, we performed an auxiliary comparison with potassium chloride (KCl), another typical ionic crystal with the same rock-salt structure as NaCl. Similar trends of HOMO localization toward the corners were observed; however, the degree of fractionalization was less pronounced in KCl due to the lower electronegativity of Cl^- relative to NaCl and the larger ionic radius of K^+, which weakens electrostatic confinement at the corners. This comparison suggests that fractional corner charge localization is a general feature of rock-salt-type ionic crystals, but its magnitude is sensitive to ionicity and lattice parameters.

4. Conclusion

In this study, we have investigated the emergence of fractional corner charges in NaCl crystal clusters by employing the DV-Xα cluster method, a real-space quantum chemical approach suitable for analyzing finite-size effects and local electronic structure. By systematically constructing one-, two-, and three-dimensional cluster models, we observed that non-integer electronic charges consistently accumulate at the corners of finite NaCl clusters, reflecting a form of topological boundary localization even in a prototypical ionic crystal.

In the one-dimensional chain model, edge-localized fractional charges emerged clearly in the density of states and local Mulliken charges, supporting the notion of charge redistribution due to the termination of periodicity. The two-dimensional square lattice clusters exhibited quantized fractional charges of approximately $-e/4$ at the four corners, consistent with theoretical predictions from higher-order topological insulator models. These results were further reinforced in the three-dimensional cuboidal

clusters, where corner-localized charges were found to be fractionalized in all directions, demonstrating the dimensional robustness of this phenomenon.

The key advantage of our approach lies in its direct quantum chemical calculation without relying on tight-binding approximations or symmetry-protected Hamiltonians. This enables a more intuitive and material-specific understanding of charge localization phenomena. Moreover, our use of the DV-Xα method allows us to track how these fractional charges emerge naturally from the electronic wavefunction and chemical bonding, emphasizing that such topological-like features can arise even in systems not traditionally considered topological insulators.

These findings bridge the conceptual gap between classical ionic crystals and modern topological materials, indicating that the concept of corner charges may be more ubiquitous than previously assumed. They also open the possibility of utilizing conventional materials to explore boundary phenomena analogous to those in topological insulators.

However, we also acknowledge several limitations in this work. The present analysis is limited to relatively small clusters due to computational constraints, and the treatment of electron correlation is within the DV-Xα framework, which may affect the quantitative accuracy of charge magnitudes. Future work should incorporate larger clusters, extended basis sets, and complementary methods such as density functional theory (DFT) to validate and refine our conclusions. Furthermore, exploring the impact of lattice distortions, defects, and external fields would deepen our understanding of the robustness and tunability of fractional corner charges.

In conclusion, this study provides compelling evidence that fractional corner charges, a hallmark of higher-order topology, can manifest in finite clusters of conventional ionic crystals. The results highlight the broader relevance of topological concepts in solid-state chemistry and motivate future investigations into real materials that host such localized electronic states for novel device applications.

Looking ahead, this computational approach can be extended to larger cluster sizes, different lattice symmetries, and other ionic systems to validate the universality of fractional charge localization. In addition, the present findings may serve as a basis for future computational and experimental exploration aimed at engineering charge-localized states in ionic and functional materials.

Acknowledgements

This work was supported by JSPS KAKENHI Grant Number 25K08676.

References

[1] W. A. Benalcazar, B. A. Bernevig, and T. L. Hughes, "Quantized Electric Multipole Insulators", *Science*, 357, 61, 2017. https://doi.org/10.1126/science.aah6442

[2] W. A. Benalcazar, B. A. Bernevig, and T. L. Hughes, "Electric Multipole Moments, Topological Multipole Moment Pumping, and Chiral Hinge States in Crystalline Insulators", *Phys. Rev. B*, 96, 245115, 2017. https://doi.org/10.1103/PhysRevB.96.245115

[3] L. Trifunovic, "Bulk-and-Edge to Corner Correspondence", *Phys. Rev. Research*, 2, 043012, 2020. https://doi.org/10.1103/PhysRevResearch.2.043012

[4] H. Watanabe and S. Ono, "Corner Charge and Bulk Multipole Moment in Periodic Systems", *Phys. Rev. B*, 102, 165120, 2020. https://doi.org/10.1103/PhysRevB.102.165120

[5] Y. Tokura, K. Yasuda and A. Tsukazaki, "Magnetic topological insulators". *Nat. Rev. Phys.*, 1, 126–143, 2019. https://doi.org/10.1038/s42254-018-0011-5

[6] Y. Ando, "Topological Insulator Materials", *J. Phys. Soc. Jpn.*, 82, 102001, 2013. https://doi.org/10.7566/JPSJ.82.102001

[7] B. A. Bernevig, "Topological Insulators and Topological Superconductors", *Princeton: Princeton University Press*, 2013. ISBN: 9781400846733

[8] M. A. Bandres *et al.*, "Topological insulator laser: Experiments", *Science,* 359, eaar4005, 2018. https://doi.org/10.1126/science.aar4005

[9] M. Zahid Hasan and Joel E. Moore, "Three-Dimensional Topological Insulators", *Annual Review of Condensed Matter Physics*, 2, 2011. https://doi.org/10.1146/annurev-conmatphys-062910-

140432
[10] G. Harari *et al.*, "Topological insulator laser: Theory", *Science*, 359(6381), eaar4003, 2018. https://doi.org/10.1126/science.aar4003
[11] N. Xu, Y. Xu and J. Zhu, "Topological insulators for thermoelectrics", *npj Quant Mater.*, 2, 51, 2017. https://doi.org/10.1038/s41535-017-0054-3
[12] A. Khanikaev, S. Hossein Mousavi, WK. Tse *et al.*, "Photonic topological insulators", *Nature Mater.*, 12, 233–239, 2013. https://doi.org/10.1038/nmat3520
[13] L. Fu, C. L. Kane and E. J. Mele, "Topological Insulators in Three Dimensions", *Phys. Rev. Lett.*, 98, 106803, 2007. https://doi.org/10.1103/PhysRevLett.98.106803
[14] M. Z. Hasan and C. L. Kane, "Colloquium: Topological Insulators", *Rev. Mod. Phys.* 82, 3045, 2010. https://doi.org/10.1103/RevModPhys.82.3045
[15] X.-L. Qi and S.-C. Zhang, "Topological Insulators and Superconductors", *Rev. Mod. Phys.* 83, 1057, 2011. https://doi.org/10.1103/RevModPhys.83.1057
[16] F. Schindler, A. M. Cook, M. G. Vergniory, Z. Wang, S. S. P. Parkin, B. A. Bernevig, and T. Neupert, "Higher-Order Topological Insulators", *Sci. Adv.*, 4(6), eaat0346, 2018. https://doi.org/10.1126/sciadv.aat0346
[17] Z. Song, Z. Fang, and C. Fang, "(d−2)-Dimensional Edge States of Rotation Symmetry Protected Topological States", *Phys. Rev. Lett.*, 119, 246402, 2017. https://doi.org/10.1103/PhysRevLett.119.246402
[18] G. van Miert and C. Ortix, "Higher-Order Topological Insulators Protected by Inversion and Rotoinversion Symmetries", *Phys. Rev. B*, 98, 081110(R), 2018. https://doi.org/10.1103/PhysRevB.98.081110
[19] J. Langbehn, Y. Peng, L. Trifunovic, F. von Oppen, and P. W. Brouwer, "Reflection-Symmetric Second-Order Topological Insulators and Superconductors", *Phys. Rev. Lett.*, 119, 246401, 2017. https://doi.org/10.1103/PhysRevLett.119.246401
[20] A. Matsugatani and H. Watanabe, "Connecting Higher-Order Topological Insulators to Lower-Dimensional Topological Insulators", *Phys. Rev. B,* 98, 205129, 2018. https://doi.org/10.1103/PhysRevB.98.205129
[21] H. Watanabe and H.-C. Po, "Fractional Corner Charge of Sodium Chloride," *Phys. Rev. X*, 11, 041064, 2021. https://doi.org/10.1103/PhysRevX.11.041064
[22] T. Nakamuro, M. Sakakibara, H. Nada, K. Harano and E. Nakamura, "Capturing the Moment of Emergence of Crystal Nucleus from Disorder", *J. Am. Chem. Soc.*, 143(4), 1763–1767, 2021. https://doi.org/10.1021/jacs.0c12100
[23] T. Ishii, K. Ogasawara and G. Sakane, "Exploring spin states and ligand field splitting in metal complexes: a theoretical analysis of spin–orbital interactions and magnetic properties", *Dalton Trans.*, 53, 7175-7189, 2024. https://doi.org/10.1039/D4DT00329B
[24] T. Ishii, S. Tsuboi, G. Sakane, M. Yamashita and B. K. Breedlove, "Universal spectrochemical series of six-coordinate octahedral metal complexes for modifying the ligand field splitting", *Dalton Trans.*, 680-687, 2009. https://doi.org/10.1039/B810590A
[25] H. Hori, S. Takemura, H. Obata and K. Ogasawara, "Prediction of $4f^7$–$4f^6 5d^1$ transition energy of Eu^{2+} in oxides based on first-principles calculations and machine learning", *Advance Sustainable Science, Engineering and Technology (ASSET)*, 2(1), 0200107-1–0200107-6, 2020. https://doi.org/10.26877/asset.v2i1.6212